

Supporting Information

High Photoluminescence Quantum Yield of 18.7% by Nitrogen-Doped Ti₃C₂

MXene Quantum Dots

Quan Xu,^{a} Lan Ding, ^a Yangyang Wen, ^a Wenjing Yang, ^a Hongjun Zhou, ^a Xingzhu Chen, ^b Jason Street, ^c Aiguo Zhou, ^d Wee-Jun Ong, ^e Neng Li, ^{b*}*

AUTHOR ADDRESS:

- a. State Key Laboratory of Heavy Oil Processing, China University of petroleum(Beijing), 102249, China
- b. State Key Laboratory of Silicate Materials for Architectures, Wuhan University of Technology, Hubei, 430070, China
- c. Department of Sustainable Bioproducts, Mississippi State University, 39762, USA
- d. School of Materials Science and Engineering, Henan Polytechnic University, 454003, China
- e. Department of Chemical Engineering, Xiamen University Malaysia, Jalan Sunsuria, Bandar Sunsuria, 43900 Sepang, Selangor Darul Ehsan, Malaysia

Table S1. The quantum yields up of the as-prepared N-MQDs and other material.

Samples	quantum yields up (%)	Ref
N-MQDs (160°C)	18.7	This paper
Ti ₃ C ₂ QDs	10	[18]
Ti ₃ C ₂ QDs	7.13	[19]
MoS ₂ QDs	4.4	[20]

Table S2. Nitrogen atomic percentage of various chemical states in the as-prepared N-MQDs (from N1s high-resolution XPS).

Samples	N-H (%)	pyrrole-like nitrogen (%)	graphitic nitrogen (%)	Ti-N (%)
N-MQDs (120°C)	65.2	34.8	0	2.5
N-MQDs (160°C)	0	51.6	45.7	2.7
N-MQDs (200°C)	0	14.2	82.8	3

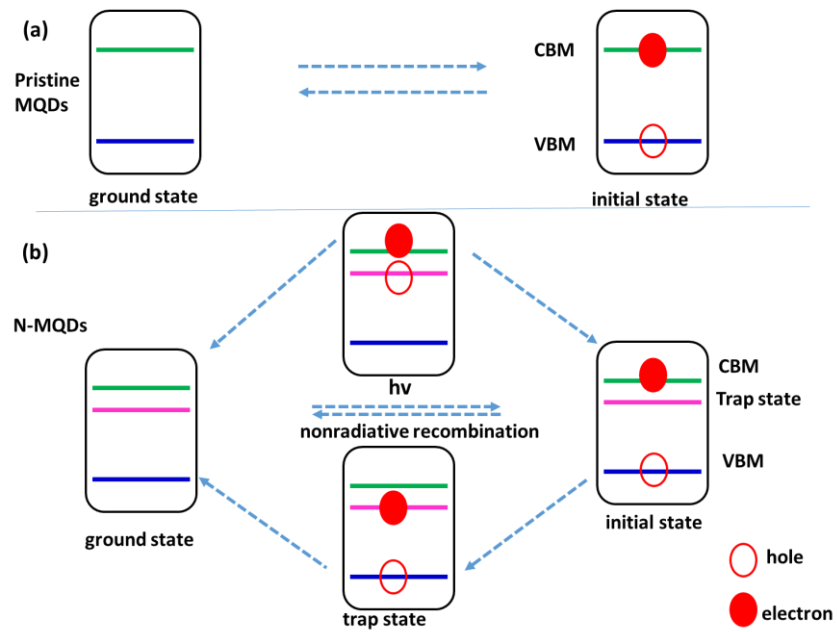


Fig. S1. Diagram of the energy levels and charge-transfer processes inside the MQDs and N-MQDs materials.

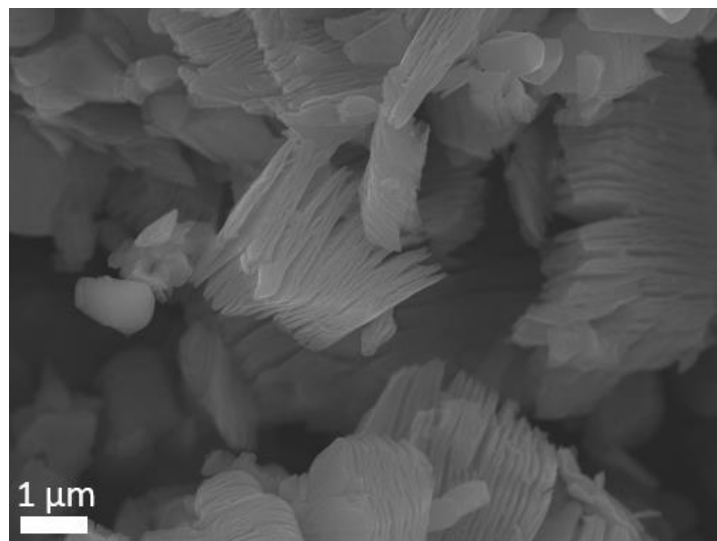


Figure S2. SEM image of the pristine Ti_3C_2 .

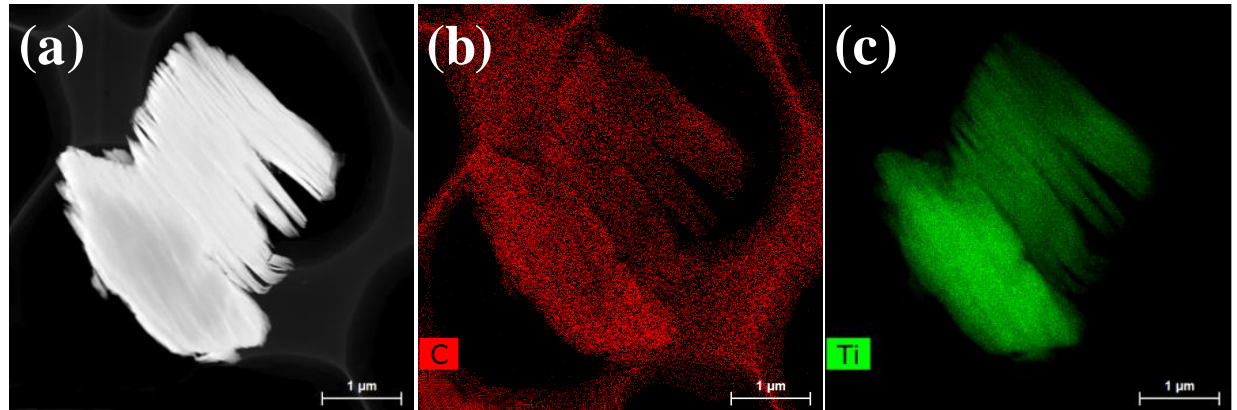


Figure S3. (a-c) TEM-EDS elemental mapping images of the pristine Ti_3C_2 sheet.

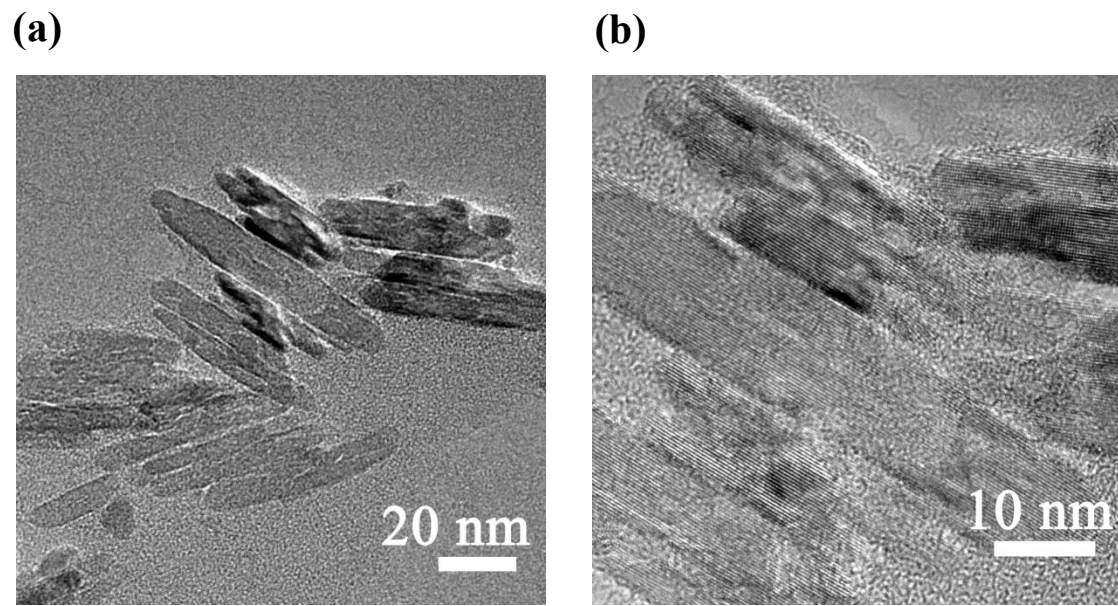


Figure S4. (a) TEM and (b) HRTEM images of the treated Ti_3C_2 (suspended in concentrated sulphuric acid in an oil bath at 100°C for 24 h).

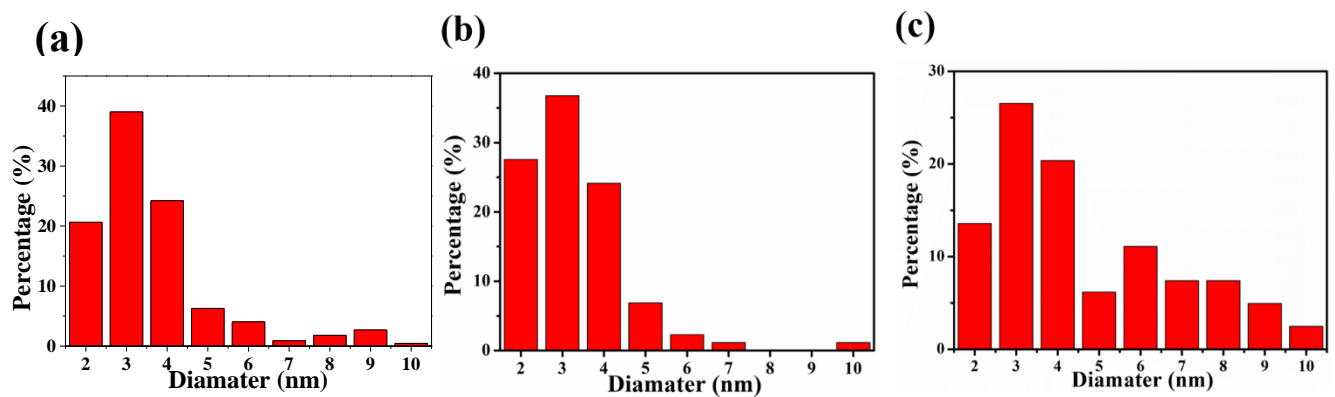


Figure S5. Diameter size distribution of N-MQDs of different hydrothermal temperature treatments: (a) 120°C, (b) 160°C, and (c) 200°C.

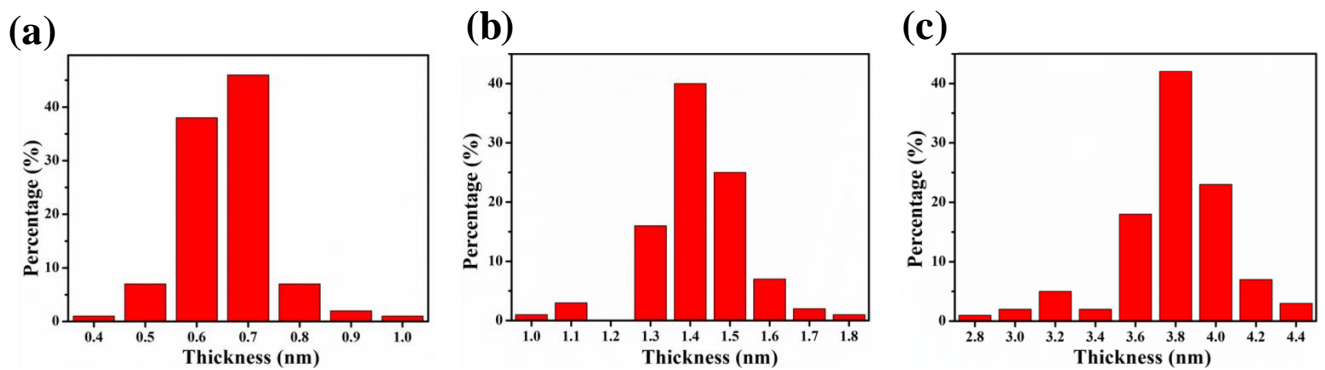


Figure S6. Thickness distribution of the prepared N-MQDs treated at (a) 120°C, (b) 160°C, and (c) 200°C.

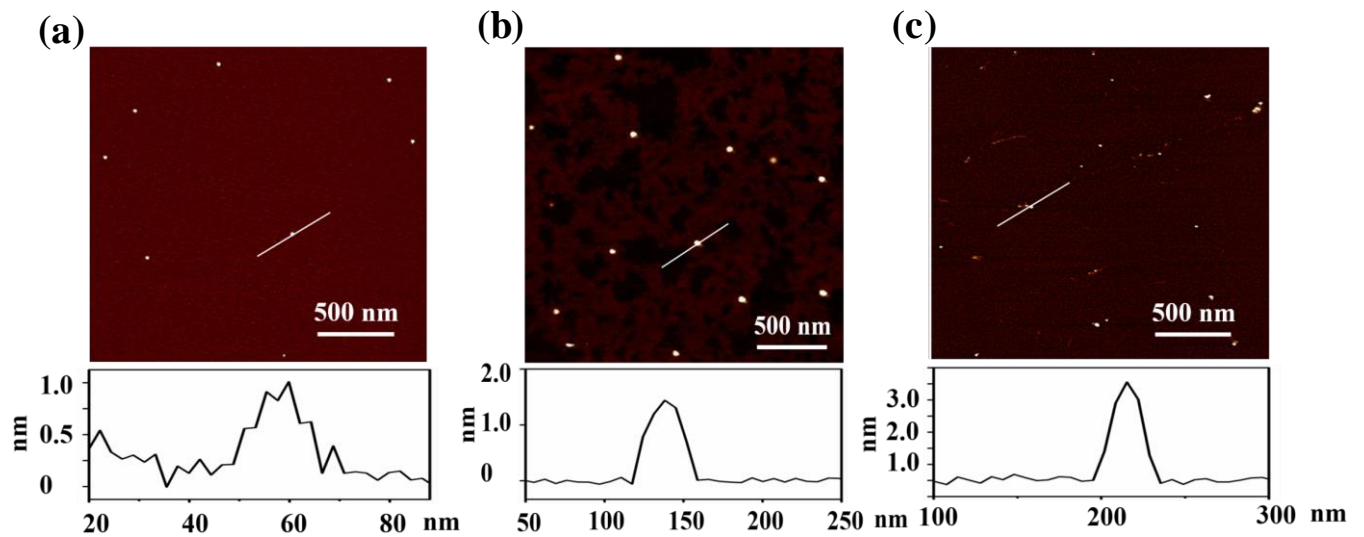


Figure S7. AFM images of the prepared N-MQDs treated at (a) 120°C, (b) 160°C, and (c) 200°C.

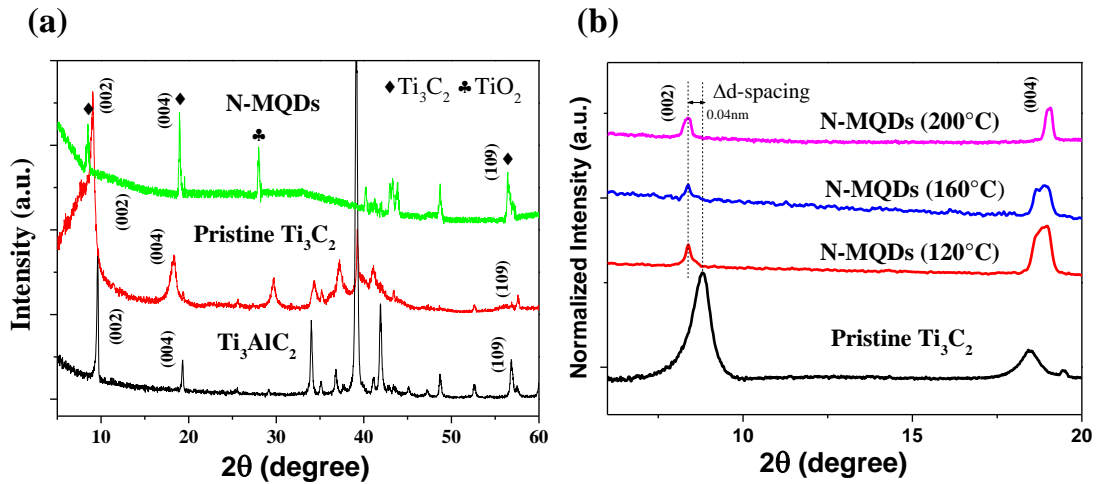


Figure S8. (a) XRD spectra of N-MQDs (160°C), pristine Ti_3C_2 and Ti_3AlC_2 . (b) Normalized GIXRD patterns of pristine Ti_3C_2 and N-MQDs.

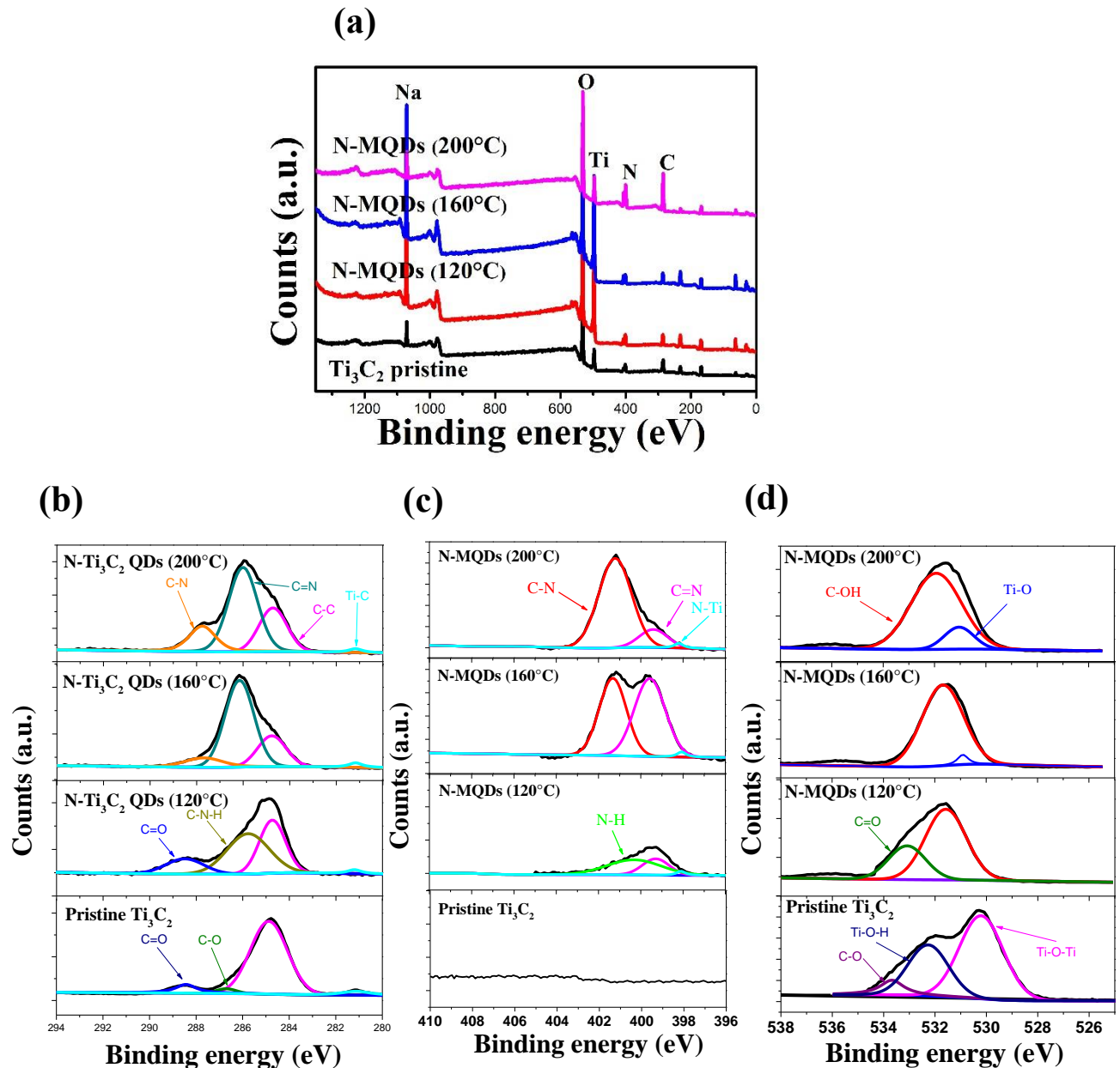


Figure S9. (a) Wide-scan XPS spectra for pristine Ti_3C_2 and N-MQDs. High-resolution XPS spectra of (b) C1s, (c) N1s, and (d) O1s XPS spectra for the pristine Ti_3C_2 and N-MQDs.

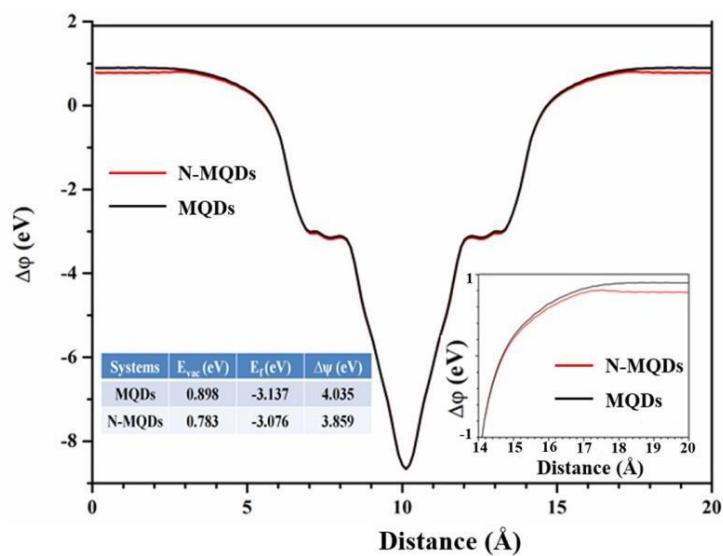


Figure S10. Work function of pristine Ti_3C_2 QDs (MQDs) and N-MQDs.

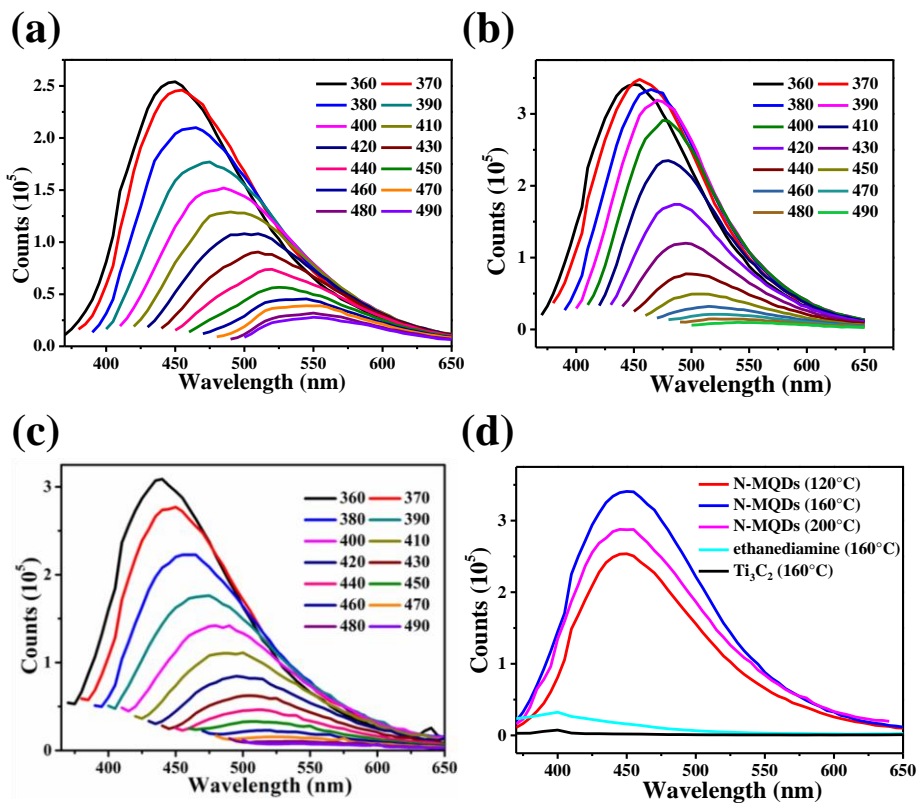


Figure S11. Photoluminescence spectra of the N-MQDs treated at different hydrothermal reaction temperatures: (a) 120°C, (b) 160°C, and (c) 200°C. (d) Photoluminescence spectra (UV light 360 nm) of N-MQDs, ethanediamine (160°C, 12h) and Ti_3C_2 (160°C, 12h, without acid treated).

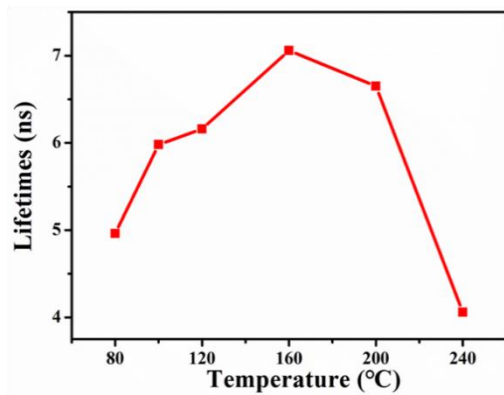


Figure S12. Lifetime of N-MQDs as a function of hydrothermal reaction temperature.

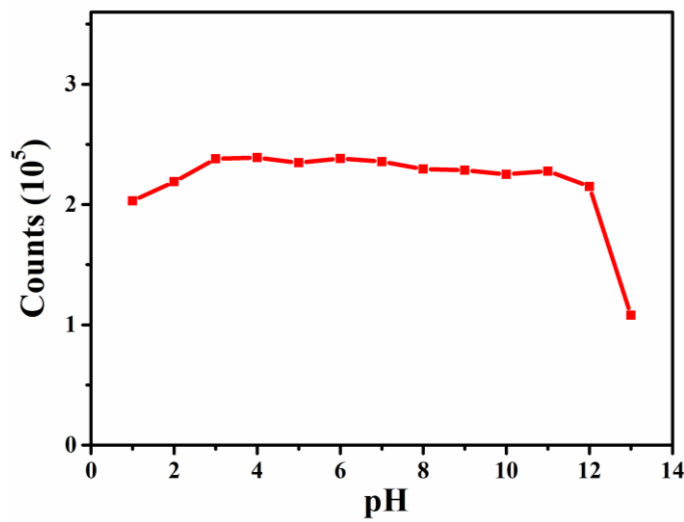


Figure S13. The fluorescence intensity of N-MQDs at 447 nm excited at 360 nm as a function of pH.

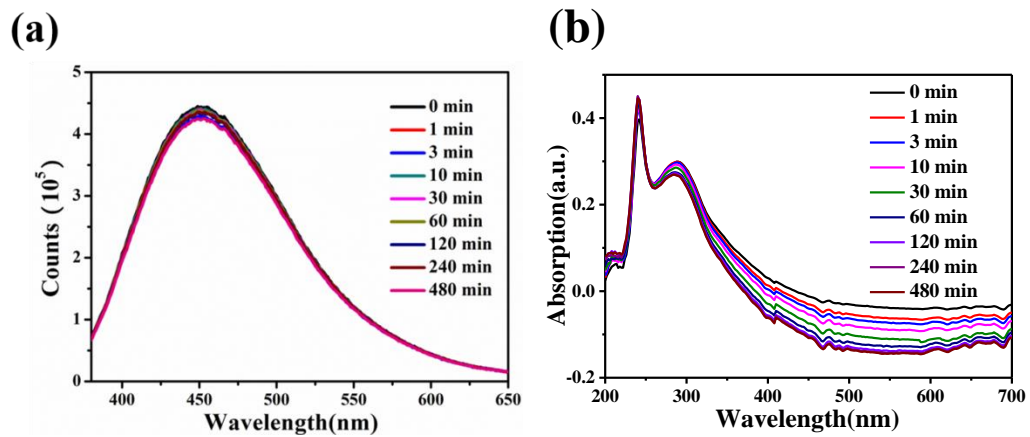


Figure S14. (a) Time-dependent fluorescence intensity and (b) absorption changes of the N-MQDs (160°C).

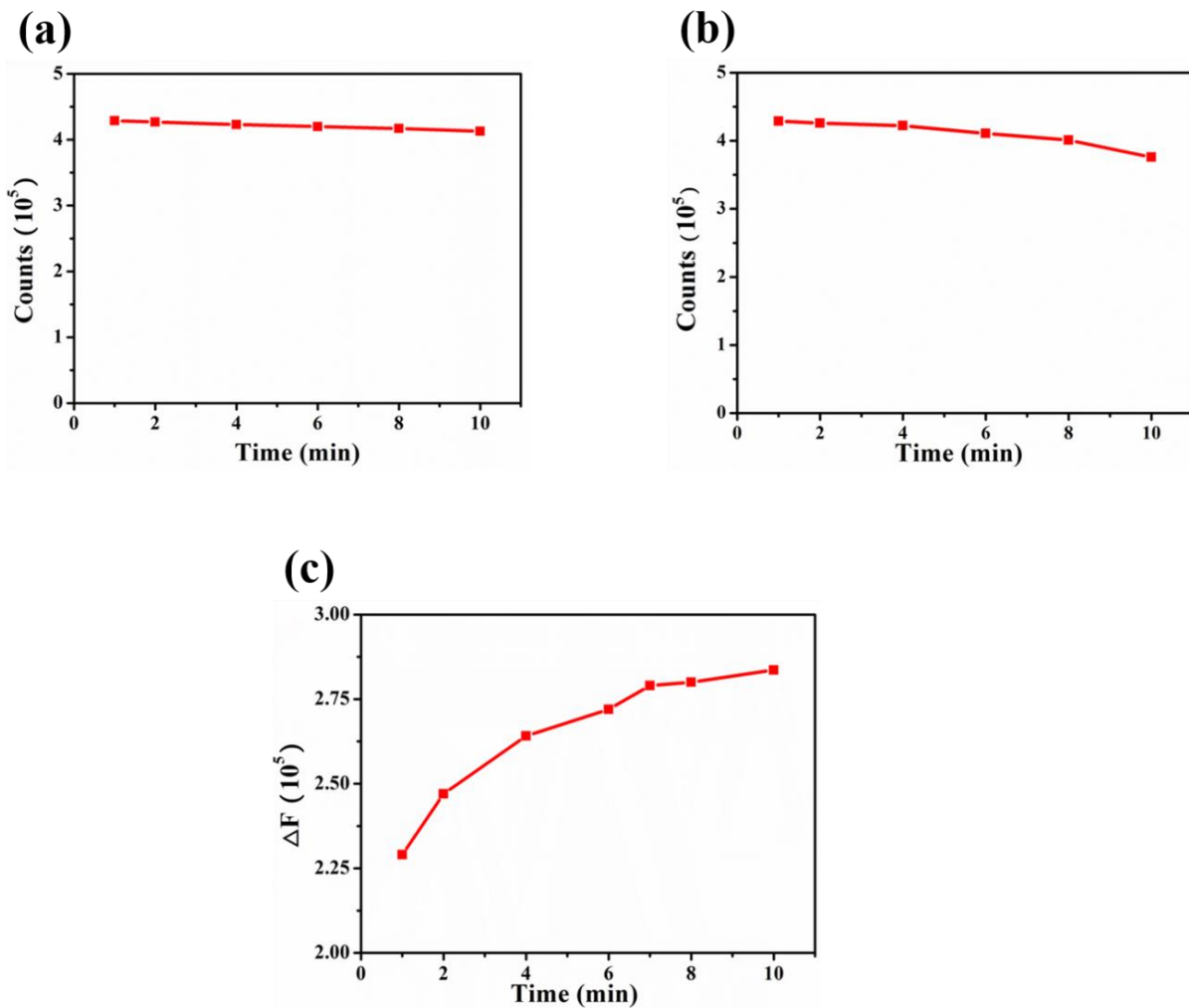


Figure S15. Time-dependent fluorescence intensity of N-MQDs in (a) 50 μM of H_2O_2 solution and (b) 50 μM of Fe^{2+} solution. (c) The degree of diversity (ΔF) of the N-MQDs with change over time in the presence of H_2O_2 (50 μM) and Fe^{2+} (50 μM) added simultaneously.